

VLBI observations of SN 2011dh: imaging of the youngest radio supernova

I. Martí-Vidal¹, V. Tudose^{2,3,4}, Z. Paragi⁵, J. Yang⁵, J. M. Marcaide⁶, J. C. Guirado⁶, E. Ros^{6,1}, A. Alberdi⁷, M. A. Pérez-Torres⁷, M. K. Argo², A. J. van der Horst⁸, M. A. Garrett^{2,9}, C. J. Stockdale¹⁰, and K. W. Weiler¹¹

¹ Max-Planck-Institut für Radioastronomie, Auf dem Hügel 69, D-53121 Bonn (Germany) e-mail: imartiv@mpifr-bonn.mpg.de

² Netherlands Institute for Radio Astronomy, Oude Hoogeveensedijk 4, 7991 PD Dwingeloo (the Netherlands) e-mail: tudose@astron.nl

³ Astronomical Institute of the Romanian Academy, Cutitul de Argint 5, RO-040557 Bucharest (Romania)

⁴ Research Center for Atomic Physics and Astrophysics, Atomistilor 405, RO-077125 Bucharest (Romania)

⁵ Joint Institute for VLBI in Europe, Postbus 2, 7990 AA Dwingeloo (the Netherlands)

⁶ Dpt. Astronomia i Astrofísica, Univ. Valencia, C/ Dr. Moliner 50, 46100 Burjassot (Spain)

⁷ Instituto de Astrofísica de Andalucía, CSIC, Apdo. Correos 2004, E-08071 Granada (Spain)

⁸ Universities Space Research Association, NSSTC, Huntsville, AL 35805 (USA)

⁹ Leiden Observatory, Leiden University, PO Box 9513, 2300RA Leiden (the Netherlands)

¹⁰ Marquette University, Milwaukee, WI, USA

¹¹ Naval Research Laboratory, Washington D.C., USA

Letter accepted for publication in Astronomy & Astrophysics

ABSTRACT

We report on the VLBI detection of supernova SN 2011dh at 22 GHz using a subset of the EVN array. The observations took place 14 days after the discovery of the supernova, thus resulting in a VLBI image of the youngest radio-loud supernova ever. We provide revised coordinates for the supernova with milli-arcsecond precision, linked to the ICRF. The recovered flux density is a factor ~ 2 below the EVLA flux density reported by other authors at the same frequency and epoch of our observations. This discrepancy could be due to extended emission detected with the EVLA or to calibration problems in the VLBI and/or EVLA observations.

Key words. ISM: supernova remnants – radio continuum: general – supernovae: general – supernovae: individual: SN 2011dh – radiation mechanisms : nonthermal

1. Introduction

Radio emission from core-collapse supernovae (CCSNe) is relatively rare. (Around 20–30% of the CCSNe are detected in radio; see, e.g., Weiler et al. 2002.) There is, indeed, only a handful of these objects for which the radio structure has been (at least partially) resolved with very-long-baseline interferometry (VLBI) observations. However, it is definitely worth monitoring any potential radio emission from this kind of events, in order to perform detailed studies of the physical conditions in the expanding supernova shocks. The case of supernova SN 1993J is the best example of such a study (see, e.g., Bartel et al. 2002; Marcaide et al. 2010; Martí-Vidal et al. 2011a; and references therein). The intense VLBI/VLA observing campaign of this supernova allowed these authors to constrain much of the parameter space of the models (density profiles of ejecta and circumstellar medium, hydrodynamical instabilities and their role in the magnetic-field amplification, energy equipartition, etc.) and to discover unexpected effects that led to the revision and extension of the standard supernova interaction model (Martí-Vidal et al. 2011a, 2011b).

SN 2011dh is a recent example of a radio-loud supernova. Located in the galaxy M 51 (distance of 7–8 Mpc; e.g., Takáts & Vinkó 2006) at the coordinates $\alpha = 13^{\text{h}} 30^{\text{m}} 05.124^{\text{s}}$ and $\delta = +47^{\circ} 10' 11.301''$ (Sárneczky et al. 2011), it was discovered with the Palomar Transient Factory project (PTF) on 2011 June 01 (Silverman et al. 2011; Arcavi et al. 2011). Radio emission

from SN 2011dh was detected just three days after its discovery, with the Combined Array for Research in Millimeter-wave Astronomy (CARMA) at 86 GHz (Horesh et al. 2011), and monitoring was also started with the Expanded Very Large Array (EVLA) and the Submillimeter Array (SMA) at several frequencies, running from 8 GHz to 107 GHz (K.W. Weiler et al., in preparation).

The expansion velocity of the shock, as estimated from the $H\alpha$ blueshift, is $17\,600\text{ km s}^{-1}$ (Silverman et al. 2011; Arcavi et al. 2011), similar to those of other supernovae of types II and Ib/c. Early X-ray emission was reported from *Swift* observations (Kasliwal & Ofek 2011). A good candidate for the progenitor star was isolated from *HST* observations (Li et al. 2011), and it shows very similar characteristics to the progenitor of the Type II-L (or spectroscopically-peculiar II-P) supernova SN 2009kr (Elias-Rosa et al. 2010).

However, the results reported in Li et al. (2011) on the progenitor of SN 2011dh conflict with more recent results reported by Arcavi et al. (2011) and Soderberg et al. (2011). Based on a detailed monitoring of SN 2011dh in X-rays (using the *Swift* and *Chandra* satellites) and radio (using the SMA, CARMA, and EVLA), Soderberg et al. (2011) report a fit to the data at all frequencies using a model of non-thermal synchrotron emission plus inverse-Compton upscattering of a thermal population of optical photons. According to these authors, SN 2011dh would match a type IIb supernova better (i.e., similar to SN 1993J), but with a compact progenitor and a shock expansion speed of

$\sim 30\,000\text{ km s}^{-1}$ (a factor ~ 2 higher than that of SN 1993J). Based on VLBI observations, Bietenholz et al. (2011) do report a barely resolved image of SN 2011dh, on day 83 after the optical discovery, with an angular radius of $0.11^{+0.09}_{-0.11}$ mas (i.e., an average expansion speed of $1.9^{+1.6}_{-1.9} \times 10^4\text{ km s}^{-1}$).

In this letter, we report on an earlier VLBI detection of SN 2011dh made at the frequency of 22 GHz, just 14 days after the discovery of the supernova. We provide a revised position of the supernova with milli-arcsecond precision, based on phase-referencing observations with a calibrator in the international celestial reference frame (ICRF). This position may be useful for improving future VLBI observations of the supernova. (Indeed, the position estimate reported here has been used in the correlation of the observations already reported in Bietenholz et al. 2011.) In the next section, we describe our observations and the calibration strategy followed in the data analysis. In Sect. 3, we report on the results obtained. In Sect. 4, we summarize our conclusions.

2. Observations and data reduction

The observations were performed on 2011 June 14 using part of the European VLBI Network (EVN) at 22 GHz. The participating antennas were Effelsberg (100 m diameter, Germany), Robledo and Yebes (70 m and 40 m, respectively, Spain), Onsala (20 m, Sweden), Metsähovi (14 m, Finland), and the MkII telescope at Jodrell Bank (25 m, United Kingdom).

The recording rate was set to 1 Gbps (dual-polarization mode), with a total bandwidth coverage of 128 MHz (divided into eight equal sub-bands for the data recording) and a two-bit sampling. The observations lasted 11 hours and 24 minutes (about 120 hours of overall baseline time), but only a total of ~ 70 hours of useful baseline time was obtained after the data correlation and calibration, mainly due to the more limited participation of some of the stations and the nondetection of fringes related to Robledo (likely related to issues in the antenna subreflector) and Metsähovi (problem with MkIV formatter).

The observations were scheduled in phase-reference mode, using the source J1332+4722 (about 0.5 degrees away from the supernova) as the main phase calibrator. Additional sources were observed as fringe finders and flux calibrators (3C286, 3C345, and J1156+295, observed every 40–50 duty cycles), as a secondary calibrator (B1333+459, observed once every six to ten cycles), and to allow the calibration of the evolution in the tropospheric delay at each station (see, e.g., Brunthaler et al. 2005 for details). Duty cycles with two different periods (90 and 120 seconds) were used in the observations, since the coherence time and the optimum on-calibrator integration time for successful detections were not known with precision. All sources were also observed in single-dish mode at the Effelsberg radio telescope to have simultaneous estimates of the total flux densities of the calibrators.

The data were correlated at the Joint Institute for VLBI in Europe (JIVE, the Netherlands) using 128 channels per sub-band and an integration time of one second per visibility. Only the parallel hand data were correlated (i.e., the LCP and RCP data), but not their cross correlations.

The data calibration was performed using the astronomical image processing system (AIPS) of the National Radio Astronomy Observatory (NRAO, USA) with standard algorithms. First, the contribution of parallactic angle and ionosphere were calibrated out. The visibility phases in the different sub-

bands were aligned by fringe-fitting¹ a scan of a strong source (3C345, in our case), following a procedure commonly known as “manual phasecal”. Then, the multiband delays and rates of the resulting visibilities of all calibrators were fringe-fitted. The resulting gains (also corrected for the tropospheric effects with the AIPS task DELZN) were then interpolated into the scans of SN 2011dh. The a priori amplitude calibration was based on the gain curves of each antenna and the system temperatures measured at each station.

After this calibration, the behavior of the visibility amplitudes was checked as a function of time (for the different baselines) and as a function of baseline length (for similar directions in Fourier space), in a search for any parts of the experiment with bad amplitude calibration. Then, edition was applied to the obvious amplitude outliers. An image of the phase-calibrator source, J1332+4722, was generated by applying phase self-calibration (every 1–2 minutes) and a later amplitude self-calibration (one solution per antenna) until convergence in the gains and the model image was achieved. The recovered flux density was compared to the flux-density measurements performed with the Effelsberg radio telescope. We obtained compatible values of the flux density between Effelsberg, $(307 \pm 93)\text{ mJy}$, and the VLBI image, $(231 \pm 10)\text{ mJy}$.

The antenna-based amplitude factors found in the imaging and self-calibration of the J1332+4722 visibilities were then applied to the SN2011dh visibilities. Finally, an image of SN 2011dh was generated from the calibrated visibilities, as described in the following section.

3. Results and discussion

3.1. VLBI detection of SN2011dh

After the calibration described in the previous section, an image of the supernova was synthesized by Fourier inversion from the space of visibilities into the sky plane. Natural weighting was applied to the visibilities, in order to improve the sensitivity of the array². We show the resulting image of the supernova in Fig. 1. Due to the limited dynamic range achieved, no further self-calibration was applied to the data to avoid the eventual generation of a spurious contribution to the flux density (see, e.g., Martí-Vidal & Marcaide 2008).

There is a clear detection of a compact source with a dynamic range of ~ 10 and flux density of $2.5 \pm 0.5\text{ mJy}$, which we identify as SN 2011dh. According to the phase-reference calibration with respect to J1332+4722, the J2000.0 coordinates of the image peak are $\alpha = 13^{\text{h}} 30^{\text{m}} 5.105559^{\text{s}} (\pm 0.000007^{\text{s}})$ and $\delta = +47^{\circ} 10' 10.9226'' (\pm 0.0001'')$. The uncertainties above contain the contribution from the error in the estimate of the calibrator position and the error inherent to the phase-referencing calibration, as estimated from Pradel et al. (2006).

The source is very compact, and we do not see any clear hint of structure on the scale of the synthesized angular resolution. Indeed, the fit of a uniform-disk model to the visibilities results in a size compatible with zero (upper limit of 0.45 mas, 1σ cutoff, for the disk radius). We notice that the maximum source size that is compatible with our observations is similar to the size of our synthesized beam (as is indeed expected in observations of compact sources with a low signal-to-noise ratio, SNR).

¹ See Schwab & Cotton (1983) for a detailed description of the global fringe-fitting (GFF) algorithm.

² With this scheme, the weight of each pixel in the Fast Fourier Transform (FFT) is inversely proportional to the scatter of the visibilities.

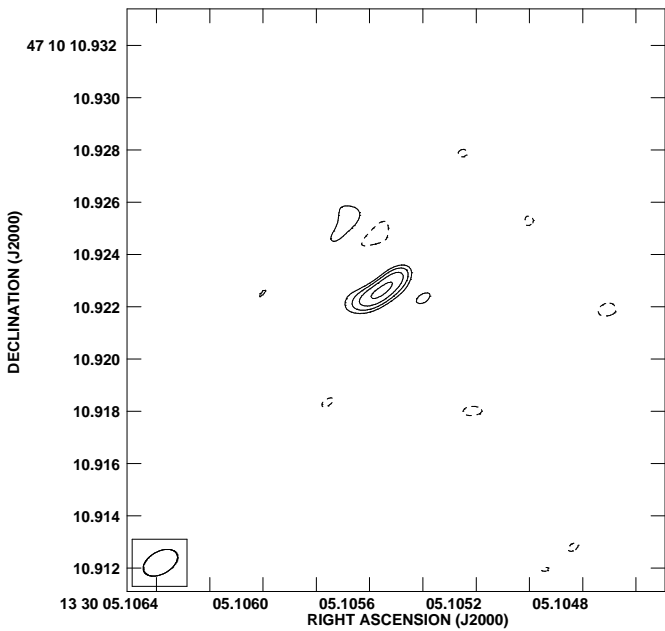


Fig. 1. Image of SN 2011dh, phase referenced to J1332+4722. The full width at half maximum (FWHM) of the convolving beam is shown at the lower-left corner. The beamsize (at the FWHM) is 1.4×0.9 mas with PA = 61 deg. (north to west). The contour levels are at -30 , 30 , 45 , 65 , and 90% of the peak flux density ($2.2 \text{ mJy beam}^{-1}$).

We therefore conclude that the angular size of SN 2011dh is well below our resolution limit at this epoch of observations. This is an expected result, since the expansion velocity in the shocks of these types of supernovae is typically a few $10\,000 \text{ km s}^{-1}$, at most. (The early ejecta velocity of SN 2001dh from the $H\alpha$ is, indeed, $17\,600 \text{ km s}^{-1}$, Silverman et al. 2011.) Assuming a distance to M 51 of 7–8 Mpc (e.g., Takáts & Vinkó 2006), a size similar to our beamwidth at this epoch would have implied a superluminal expansion. However, it is intriguing that, even though the emission comes from a very compact region at this epoch, we are unable to recover the total flux density measured with the EVLA by Soderberg et al. (2011). The lack of flux density in our VLBI observations may come either from a contribution from an extended source in the EVLA observations or from calibration biases in the VLBI (and/or EVLA) data, as discussed in Sect. 3.2.

3.2. VLBI vs. EVLA flux density

A systematic difference between the single-dish flux density of a source and the total recovered flux density in a VLBI-synthesized image is quite common. This effect takes place at all VLBI observing frequencies (with varying strength, but typically ranging from 10 to 20% at most), and is due to either a limited coherence in the correlation or to extended components in the sources that are resolved out in the VLBI fringes. However, it must be noticed that the flux density of SN 2011dh reported in Soderberg et al. (2011) implies a flux density of about 5 mJy at 22 GHz at the epoch of our observations (see their Fig. 3). This value is a factor 2 above the recovered flux density in our observations. The ratio of single-dish-to-VLBI flux density of SN 2011dh should be similar to that of J1332+4722, since the instrumental effects in the VLBI observations should be very

similar in both sources. As a result, the Effelsberg-to-VLBI flux-density ratio of the calibrator, J1332+4722, should also be similar to the EVLA-to-VLBI flux-density ratio for SN 2011dh. This similarity should allow us to estimate the amount of lost flux density in the VLBI image of SN 2011dh, and to compare it to the extra recovered EVLA flux density. However, the uncertainty in the flux-density measurement at the Effelsberg radio telescope is so high that such a comparison gives no statistical significance. The flux density of J1332+4722 recovered with the Effelsberg radiotelescope is 1.33 ± 0.45 times higher than that recovered in the VLBI image. Therefore, the relative amount of flux-density loss in the VLBI image of SN 2011dh seems to be slightly larger than (although still compatible with) the one found in the image of the phase-reference calibrator. Nevertheless, the level of significance for this statement is very low.

It must also be noticed that Bietenholz et al. (2011) report a VLBI (VLBA + GBT + Effelsberg) peak intensity for SN 2011dh of only 0.63 mJy at 22 GHz (on day 83 after the optical discovery) using the same phase calibrator (J1332+4722). This peak intensity is also lower than what would be expected from the extrapolation of the model reported in Soderberg et al. (2011).

In addition to the well-known loss of flux density in VLBI images, caused mainly by the resolution of extended emission, there is an additional loss of flux density from the effect of atmospheric turbulence in phase-referenced observations (Martí-Vidal et al. 2010). To estimate the atmospheric contribution to the flux-density loss in our VLBI observations, we measured the total flux density in the image of B1333+459, phase-referenced to J1332+4722, and compared it to the total flux density in the image obtained from the self-calibrated visibilities of B1333+459. The observed flux-density loss in B1333+459 due to phase referencing is $\sim 40\%$, which is within a factor 2 of the loss predicted in Martí-Vidal et al. (2010) for the VLBA ($\sim 25\%$, as computed from their Eq. 4). These results indicate a similar performance of the EVN and the VLBA in phase-referencing observations, even using a very small subset of the EVN in our observations (only four stations had useful detections; see Sect. 2) and a higher observing frequency. If Eq. 4 in Martí-Vidal et al. (2010) is used to estimate the flux-density loss of SN 2011dh due to phase referencing, the result is only $\sim 2\%$ (using the constants reported in that publication, which are based on VLBA observations) or $\sim 3.5\%$ (if we calibrate Eq. 4 using our estimated flux-density loss of B1333+459, phase-referenced to J1332+4722). In any case, the expected flux-density loss of SN 2011dh due to phase referencing (based on Eq. 4 of Martí-Vidal et al. 2010) is very small, given the small separation from its phase calibrator (about 3.4 times smaller than the distance between B1333+459 and J1332+4722).

In case that the missing flux density in our SN 2011dh VLBI observations (and in those reported by Bietenholz et al. 2011) was not completely due to instrumental limitations (no robust conclusion can be extracted only from our data), such a loss might also be related to a contribution of extended emission (e.g., from the background galaxy, from the continuum of the whole region, or even from the supernova environment) in the EVLA flux densities reported in Soderberg et al. (2011). We note, though, that such a contribution from an extended component in the supernova would imply that there is extended emission as strong as what comes from the (still compact) expanding shock, and this would thus conflict with the model reported in Soderberg et al. (2011), which assumes that all the emission detected with the EVLA comes from interaction of the expanding shock (with an expansion velocity of $\sim 30\,000 \text{ km s}^{-1}$).

4. Summary

We report on the VLBI detection of SN 2011dh at 22 GHz using a subset of the EVN array. The observations took place 14 days after the discovery of the supernova. Therefore, this is the VLBI image of the youngest radio-loud supernova. The source is very compact, with a size compatible with zero and upper bound of 0.45 mas for the radius of a uniform-disk model fitted to the visibilities).

We provide revised coordinates for the supernova with milli-arcsecond resolution and linked to the ICRF. The recovered flux density is a factor ~ 2 below the flux density reported in Soderberg et al. (2011), at the same frequency and day as our observations. Such a difference may indicate a contribution by extended emission in the EVLA flux densities or calibration problems in the VLBI and/or the EVLA observations. Further VLBI observations of this supernova will be decisive in helping resolve this conflict.

Acknowledgements. The European VLBI Network is a joint facility of European, Chinese, South African, and other radio astronomy institutes funded by their national research councils. We acknowledge the EVN chair and related staff for the swift answer and scheduling of the VLBI observations. The single-dish flux densities reported are based on observations with the 100-m telescope of the MPIfR. This research has been partially supported by projects AYA2009-13036-C02-01 and AYA2009-13036-C02-02 of the MICINN and by grant PROMETEO 104/2009 of the Generalitat Valenciana. E.R. was partially supported by the COST action MP0905 “Black Holes in a Violent Universe”.

References

- Arcavi I., Gal-Yam A., Yaron O. et al. 2011, arXiv:1106.3551
 Bartel N., Bietenholz M.F., Rupen M.P. et al. 2002, ApJ, 581, 404
 Bietenholz M. F., Brunthaler A., Bartel N., et al. 2011, ATel, # 3641
 Brunthaler A., Reid M.J., & Falcke H. 2005, ASPC, 340, 455
 Elias-Rosa N., van Dyk, S.D., Li W., et al. 2010, ApJ, 714L, 254
 Horesh A., Zauderer A., & Carpenter J. 2011, ATel, #3405
 Kasliwal M.M. & Ofek E.O. 2011, ATel #3402
 Li W., Filipenko A.V., & van Dyk S.D. 2011, ATel #3401
 Marcaide J.M., Martí-Vidal I., Alberdi A., et al. 2010, A&A, 505, 927
 Martí-Vidal I., & Marcaide J.M. 2008, A&A, 480, 289
 Martí-Vidal I., Ros E., Pérez-Torres M.A., et al. 2010, A&A, 515, A53
 Martí-Vidal I., Marcaide J.M., Alberdi A., et al. 2011a, A&A, 526A, 143
 Martí-Vidal I., Pérez-Torres M. A., & Brunthaler A. 2011b, A&A, 529A, 47
 Pradel N., Charlot P., & Lestrade J.-F. 2006, A&A, 452, 1099
 Sárneczky K., Szalai N., Kun M., et al. 2011, ATel #3406
 Schwab F.R., & Cotton W. D. 1983, AJ, 88, 688
 Shepherd M.C., Pearson T.J., & Taylor G.B. 1994, BAAS, 26, 987
 Silverman J.M., Filippenko A.V., & Cenko S.B. 2011, ATel #3398
 Soderberg A.M., Margutti R., Zauderer B.A., et al. 2011, arXiv:1107.1876
 Takáts K. & Vinkó J. 2006, MNRAS, 372, 1735
 Weiler K.W.W., Panagia N., Montes, M.J. et al. 2002, ARA&A, 40, 387